International Journal of Engineering Trends and Technology
ISSN: 2231–5381 / https://doi.org/10.14445/22315381/IJETT-V72I2P119

Volume 72 Issue 2, 178-189, February 2024
© 2024 Seventh Sense Research Group®

Original Article

Vertex Bar Tool Design for Decreasing Earring Defects

Wiriyakorn Phanitwong

Department of Industrial Engineering, Rajamangala University of Technology Rattanakosin, Nakhon Pathom, Thailand.

Corresponding Author : wiiriyakorn.pha@rmutr.ac.th

Received: 26 September 2023 Revised: 12 January 2024 Accepted: 14 January 2024 Published: 03 February 2024

Abstract *- The deep drawing process is a major sheet metal process used in various industrial fields, such as automobile, aerospace, computer and electronics, household utensils, and medical equipment industries. The earring defect is the main barrier to decreasing the formability, production cost, and time requirements. In this research, the so-called vertex bar tool (VBT), comprising a vertex bar (VB) die and vertex bar blankholder (VB blankholder), was proposed to decrease earring defects. The finite element method (FEM) was used to predict material flow direction within the designed tool to illustrate the principle of VB. The results demonstrate that the VB die and VB blankholder could reduce the flat top die's non-axisymmetric material flow characteristic and asymmetry during the deep drawing process. Furthermore, the workpiece thickness measured during the deep drawing process using the VB die and VB blankholder in a direction along the plane at 0°,45°, and 90° to the rolling direction were more uniform than those obtained by conventional die application implemented at the same angles in a direction along the plane. The VB die, and VB blankholder design proposed in this study fulfilled the hypothesized purpose. Therefore, using proper VB die and VB blankholder application, the earring defect could be decreased to 1.6 mm, denoting a decrease of approximately 55.55%.*

Keywords *- Anisotropy, Cylindrical component, Deep drawing process, Finite element method, Vertex bar.*

1. Introduction

Sheet-forming processes, such as bending, deep drawing, and cutting processes, are commonly used in the automobile and aerospace industries [1]. During such processes, the finite element method (FEM) is used to improve the increase in formability and quality. Moreover, FEM contributes to eliminating major defects, such as fracture, earring, and wrinkle deformations [2–8]**.** In this study, FEM was used to reduce the distortion of the earrings that happens during the deep drawing process. This process is commonly used in industrial applications, such as automobile, aerospace, and household utensils manufacturing. The final steps ensuring good quality on a more complex profile are low cost compared to the rest of the process [9–11]. A deep drawing process for square cups is optimized based on the process parameters of AA5182 [9] and lightweight materials for the automobile industry [10]. Developing a drawing bead design that is properly optimized based on the deep drawing depth, diameter die, and initial part has been proposed in the literature [11]. The thinning is the most commonly occurring defect in the deep drawing process, causing crack deformations. A hybrid composite material manufactured using steel with fiber-reinforced plastics was investigated in [13]. A technique developed for micro deep-drawn parts was applied to general deep-drawn parts in the literature [15–18]; for example, a multi-layered process was conducted using an ultra-thin copper foil to obtain a conical part [15].

Cylindrical cup shapes are widely used in sheet metal forming processes in many industries. Therefore, this process has been continuously developed via experimental and FEM simulation studies. Major defects, such as fractures, earrings, and wrinkle deformations, must be prevented. The limit drawing ratio (LDR) defines the increase in the multi-draw radius design and zoning lubricant die application, which has been validated in several previous studies. The flange winkle technique model on total deformation has been used together with a macro-texture blankholder [19–22].

A couple of studies have reported the results of the buckling behavior [23, 24]. The friction coefficient is the most important parameter characterizing deformation behavior. A high friction coefficient causes fracture deformation, while an unbalanced friction coefficient results in earring deformation. Many techniques using lubricants are proposed to decrease friction [25]; for example, liquate, solid, and air lubricants, for instance, are applied over the surface where the workpiece and die make contact [30, 31]. Moreover, numerous techniques use newly designed dies and blank holders, such as the multi-draw radius design, macro-structure and micro-structure tools for vertex bar tools, etc. [26-29]. However, in existing studies, the decreases in earring defects are still mainly limited. In addition, the method to decrease the earring defect is usually complex, involving the application of the Vertex Bar Tool (VBT) technique.

This is an open access article under the CC BY-NC-ND license (http://creativecommons.org/licenses/by-nc-nd/4.0/)

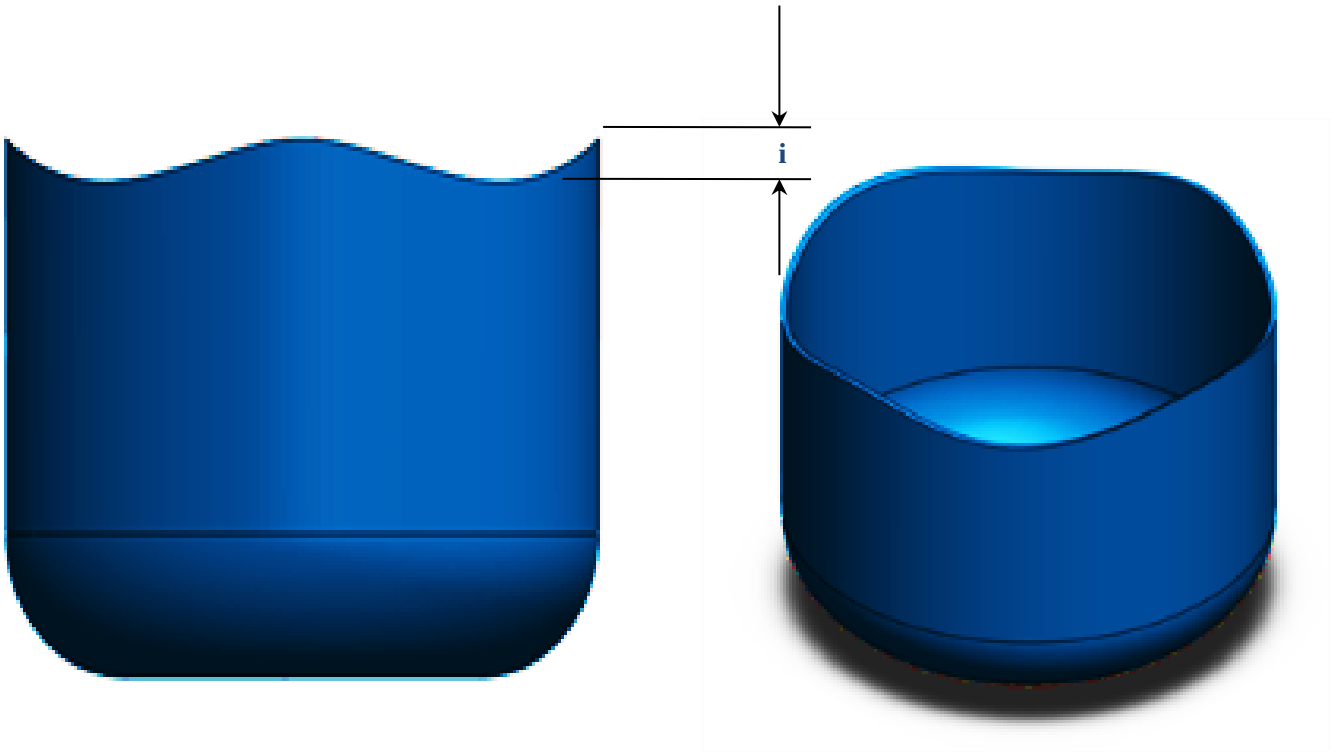

Fig. 1 Cylindrical model of the deep drawing process: (i) earring defect

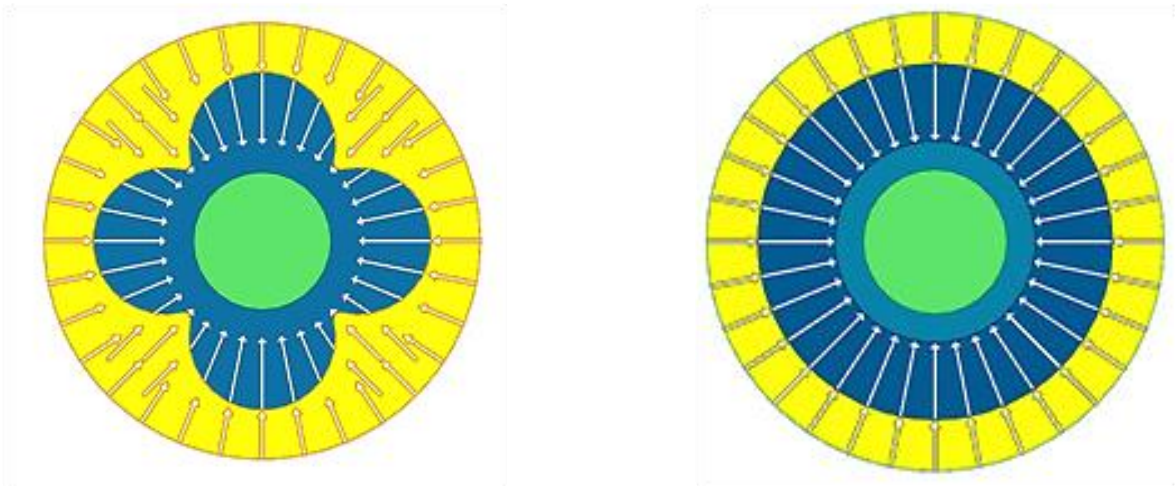

(a) **(b)**

Fig. 2 Principle of VB die and VB blankholder based on the material flow characteristic: (a) Conventional die (b) Vertex bar tool.

In the present research, therefore, a new approach is proposed to decrease the earring defect based on plastic strain ratio(R-value), which is the basic mechanical property affecting the material flow on the flange. However, in the proposed design of the VB die and VB blank holder, it is recommended that the VB die and VB blank holder be positioned at 45° to the rolling direction and flat die and flat blank holder at 90° to the rolling direction. The results obtained after applying the VB die, and blank holder were compared with those obtained with the conventional die, illustrating that the earring defect could be decreased.

2. Defects on the Deep Drawing Process

2.1. Earring Defect in Deep Drawing Process

The rolling direction greatly affects the material deformation characteristics. The rolling direction causes defects in the workpiece. An important flaw commonly occurring on deep drawing workpieces is the ear-shaped defect. Therefore, the shape of the workpiece after deep drawing deformation will have earring defects. Positions with greater height are the 0°and 90°angles with respect to the rolling direction, while the position with less height is

45°angle with respect to the rolling direction, as shown in Figure 1. Figure 2 compares the material flow characteristics between the conventional die and the Vertex Bar Tool (VBT). A different material flow causes the material flow to be unequal, as shown in Figure 2a. The anisotropy property is included in the basic deformation theory, which is the cause of the earring defect occurring on the final part. The present research proposes the Vertex Bar Tool (VBT) to improve the die design. VB decreases the anisotropy by controlling the friction on the initial part around the contract area based on the pressure between the die with the initial part and the blank holder with the initial blank. Therefore, the material flow fluctuations are decreased, effectively decreasing the earring defects, as shown in Figure 2b. The height values at positions 0°, 45°, and 90° to the rolling direction are approximately the same.

3. Materials and Methods

3.1. Die Components

Figure 3a shows the mold components used in the deep drawing process, comprising a punch, die, and blank holder. As the first step, the blank holder moves down to press the workpiece against the die. After that, the punch will move down to press the initial blank, modifying the initial blank shape. The die shape is symmetrical around the axis and that of the initial blank. However, the initial blank is not symmetrical because the plastic strain ratio (R-value) at angles 0°, 45°, and 90° are unequal. This is due to the deformations that occur as the workpiece is rolled into sheet metal, which is a forming process required as a preliminary step in the previous process. The objective of the rolling process is to obtain a workpiece with a desired thickness. The rolling direction is observable on the workpiece.

The simulation is conducted considering the JIS standard medium carbon steel (SPCC) with a thickness of 0.5 mm in this study. Important basic mechanical material properties are the constitutive equation, Poisson's ratio, %elongation, Young's modulus, and ultimate tensile strength, the values for which are reported in Table 1. Plastic strain ratio (R-value) at angles of 0°, 45°, and 90° must be known for the deep drawing process for conducting an accurate finite element simulation. In this research, the AutoForm R10 (C. Meicher & Co. (Thailand) Ltd.) software is used for the Finite element method (FEM)simulating the deep drawing process. The simulation must have a model with the IGES extension, which can be obtained using the program cimatron3 (3D Systems INC., Givat Shmuel, Israel). When designing the vertex bar tool, it is crucial to consider the flow behavior of the material. Accordingly, the values of the variables height (h), radius (R), wide slot (Ws), and wide (w) used in this research are shown in Figure 3. Using lubricants is standard; thus, the friction force value during the normal molding process is 0.1. The experimental workpiece (initial blank) is defined as elastic-plastic, while the mold parts (punch, die, press plate) are defined as rigid. The shape of the element is triangular with 3 nodes. The number of elements used in the FEM analysis is approximately 3700.

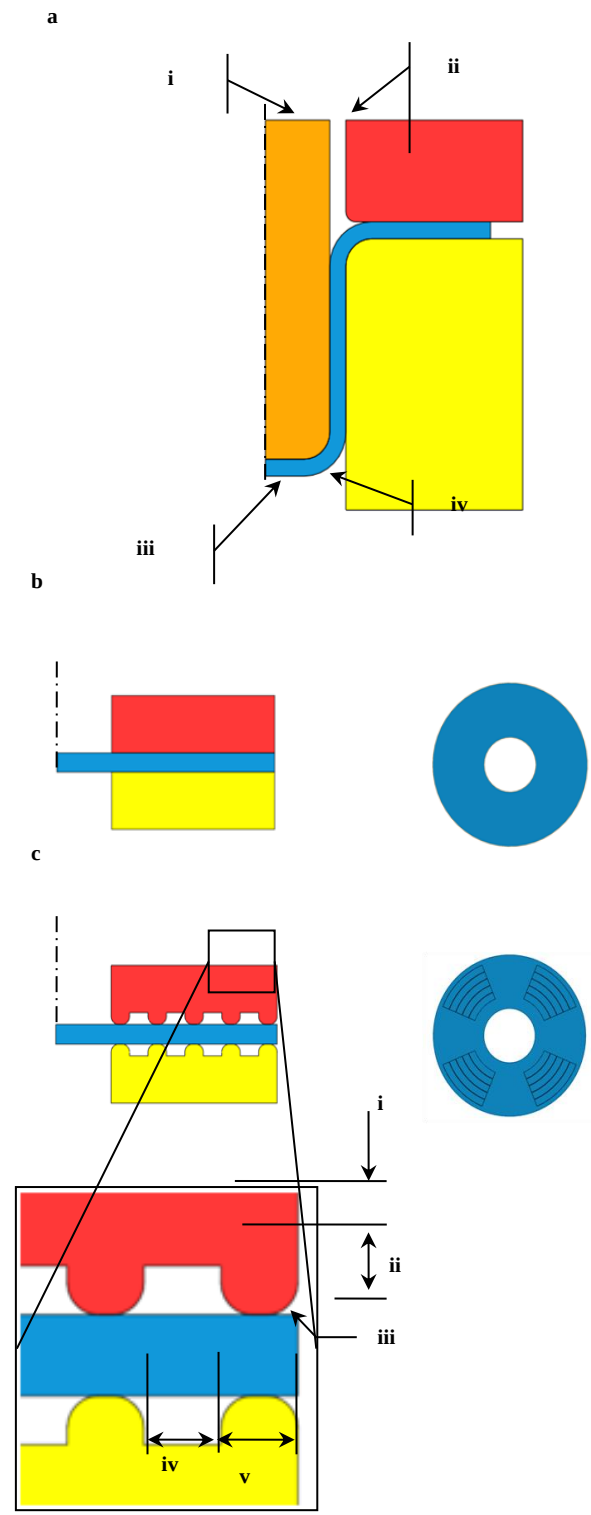

Fig. 3 Approach used to create the vertex bar tool for a deep drawing process: (a) Deep drawing model with (i) Punch, (ii) Blank holder, (iii) Workpiece, and (iv) Die. (b) Conventional die. (c) Vertex bar tool, (i) Groove Height, (ii) Material thickness, (iii) Radius, (iv) Wide slot, (v) Wide.

Table 1. FEM simulation and experimental conditions.

Object type	
Sheet material	elastic-plastic
Tool (punch, die, blankholder)	rigid
Sheet material	
Medium carbon steel	SPCC, JIS
Thickness (t)	0.5 mm
Ultimate tensile strength	317 MPa
Young's modulus	208 GPa
% elongation	51
Poisson's ratio	0.33
Constitutive equation	$\bar{\sigma} = 554.43\bar{\varepsilon}^{0.23} + 208$
Blank holder force	Gap type
Plastic strain ratio (R-value)	
0°	2.1
45°	1.9
90°	2.6
Blank diameter	90 mm
Tool geometry	
Punch radius	8 mm
Punch diameter	40 mm
die radius	8 mm
Detail structure tool	
Groove Height (h)	3 mm
Radius (R)	0.2 mm
Wide slot (W_s)	5 mm
Wide (w)	0.5 mm
Friction coefficient (μ)	0.1

4. Results and Discussion

4.1. Comparison of Material Flow Analysis Results between Conventional Die, VB Die, and Blankholder Application

The material flow can be illustrated using a FEM simulation in both the conventional die case and VB and VB blank holder case. The comparison of material flow between the conventional die and VB die, as well as blank holder applications is shown in Figure 4. The material flow varied during the deep drawing process, with a die stroke of approximately 5 mm, as shown in Figures 4-a1 and 4-a2. In the case of a conventional die, a fast flow value is observed.

On the contrary, a slow value is observed in the VB die and blank holder case. These simulation results are coherent with the deep drawing theory [1]. The non-axisymmetric material flow exhibited more variations with a die stroke of approximately 15 mm, as shown in Figures 4-b1 and 4-b2. In the case of a conventional die, an unsmooth flow value is observed around the flat top die, having the appearance of a wave. On the contrary, a smooth flow value is observed around the flat top die in the case of the VB die and blank holder. With a die stroke of approximately 25 mm, as shown in Figures 4-c1 and 4-c2, the effects of the material anisotropy property on material flow exhibited more variations. They affected the initial blank shape on the top. In the case of a conventional die, an obvious unsmooth flow is observed around the connection point between the die surface and circumference, having a more pronounced wave appearance. Due to the uneven flow, the shape of the workpiece sheet changed from a circle to a square. On the contrary, in the case of the VB die and VB blank holder, a smooth flow value is observed around the connection point between the die surface and circumference. Due to the uniform flow, accordingly, the workpiece shape does not change from a circle to a trapezoid.

With a die stroke of approximately 35 mm, as shown in Figures 4-d1 and 4-d2. In the case of a conventional die, the material anisotropy property affected material flow more significantly, denoting a greater difference between the results obtained with 0° and 90° with respect to the rolling direction and those obtained with 45° with respect to the rolling direction. Accordingly, the initial blank shape changed significantly from a circle to a trapezoid.On the contrary, a continuous smooth flow value is obtained in the case of the VB die and blank hoined, and the workpiece shape remains circular.

Moreover, the material flow characteristics remain the same until the material flows through the die radius with a die stroke of approximately 45 mm, as shown in Figures 4-e1 and 4-e2. In contrast, in the case of the VB die and blankholder application, the effects of the anisotropy property of the material to flow unsmooth material were continuously compensated by the VB die and blankholder. These results demonstrated that by using VB die and blankholder application, the effects of the material anisotropy property on the flow causing unsmooth material surfaces could be compensated during step-by-step during the deep drawing process, which resulted from the non-axisymmetric characteristic of material flow on the flat top die. Subsequently, cup wall stretching can be prevented, and earring defects can be decreased**.**

4.2. Comparison of Material Flow Analysis Obtained with the VB Die and Blankholder between Excessive and Inadequate Case Applications

As mentioned in the previous section, the anisotropy property, related to the VB parameter, affects material flow. Therefore, the designed VB die and blankholder are influenced by the anisotropy property of the material flow; accordingly, the position of the designed VB with a fast velocity is at 45° to the rolling direction.

The different variable is the groove height (H). Figure 5-1 depicts higher groove examples, while Figure 5-2 depicts shorter groove examples. The material flow values remained close during the deep drawing process, with a dying stroke of approximately 5 mm, as shown in Figures 5-a1 and 5-a2.

With a die stroke of approximately 15 mm, as shown in Figures 5-b1 and 5-b2, the non-axisymmetric material flow showed more difference. In the case of a higher groove, a more

unsmooth flow value is observed compared to that observed with a shorter groove around the flat top die, having the appearance of a square.

With a die stroke of approximately 25 mm, as shown in Figures 5-c1 and 5-c2, the effects of the material groove height on material flow showed more difference, which was prominent on the initial blank shape at the top. When using a flat-top die, the material struggles significantly to flow in the die. The velocity profile assumes the appearance of a starburst, affecting the fracture deformation around the punch radius.

On the contrary, in the VB die and blank holder case, an unsmooth flow value is observed around the connection point between the die surface and circumference. Here, the velocity profile assumes the appearance of a starburst again, with a smaller magnitude than that observed under the higher groove condition. With a die stroke of approximately 35 mm, as shown in Figures 5-d1 and 5-d2, in the case of a higher groove, the groove height significantly hindered the material flow at 45° with respect to the rolling direction.

However, it partially allowed material flow at 0° and 90° with respect to the rolling direction. Subsequently, the workpiece fractured. On the contrary, in the case of the VB die and blank holder, a continuous unsmooth flow value is observed.

Moreover, different flow is observed at 45° to the rolling direction, with the material flow characteristics remaining the same until the entire material flows through the die radius with a die stroke of approximately 45 mm.

This is shown in Figure 5-e2. Contrarily, in the cases of higher and shorter groove applications, the effects of the material anisotropy property on flow characteristics causing an unsmooth material surface were continuously compensated by the higher groove. According to the explanation above, a contract pressure relationship occurs between the die and the material. As demonstrated in Figures 6-a1, 6-b1, 6-c1, and 6-d1, with a die stroke of roughly 25 mm, there is a noticeable variation in the impact of material groove height on contact pressure. The original composition makes this very evident. The suitable contract pressure value is shown by the initial blank form at the top, which is at a 45-degree angle and has the appropriate VBT value. Conversely, a VBT A VBT Shorter groove that is too narrow causes an uneven material flow, while a higher groove produces excessive contract pressure that prevents the material flow.

A smooth top die will make it extremely difficult for the material to flow into the die. As a result, as seen in Figures 6-a2, 6-b2, 6-c2, and 6-d2, the blank form at the top created in a die stroke of 35 mm clearly exhibits varied workpiece shapes.

The results depicted that the final deep drawn parts could be formed by conventional die, VB die, and blank holder, which were applied in both cases. All die designs are depicted in Figures 7a, 7b, 7c, and 7d. However, the VB die, and blankholder applications with grooves showed greater earring defects than those observed with VB die and blankholder type appropriate applications.

Accordingly, the erring defect position changed from 0° and 90° in the rolling direction to 45° in the rolling direction of the conventional die. Therefore, the anisotropy property is confirmed to be affected by the rolling direction.

Groove height on the die and blankholder is an important parameter to control material flow on a flat top die. Therefore, choosing the appropriate variable values can reduce the earring defect problem. These results demonstrate that deep-drawn parts could be achieved using VB die and blankholder application.

FLD is the basic deep drawing theory [1], which clearly demonstrates the fracture characteristics along the workpiece circumference by FEM simulation results, as shown in Figures 7a-2 and 7a-3. The result agreed well with deep drawing theory [1].

On the contrary, when using the VB die and blankholder application, we observed that the deep drawn part could be obtained using the VB die and blankholder type appropriate application, as shown in Figures 7b-2 and 7b-3. However, using the VB die and blankholder type higher groove, the final deep drawn part could not be achieved owing to fracture defect occurring around the punch radius. The characterized fracture was the basis of FLD, as shown in Figures 7c-2 and 7c-3.

Moreover, using the VB die and blankholder type shorter groove, the final deep-drawn part could not be achieved owing to the earring defect. The detected two earring defects were the basis of FLD, as shown in Figures 7d-2 and 7d-3. Owing to the material anisotropy property, the VB die and blank holder is differently designed at 0° and 90° to the rolling direction compared to the design implemented at 45° to the rolling direction.

Figures 4c1 and 5c2 show that the conventional die, VB die, and blankholder-type shorter grooves resulted in earring defects because of non-axisymmetric material flow.

The material flow analyses show the non-axisymmetric on the flat top blank, which causes cup wall stretching and fracture deformation. On the other hand, after selecting the appropriate variables, the flow material characteristic can be controlled throughout the workpiece, reducing the earring defect, as shown in Figure 4c2. However, the flow material characteristic is too complex, which will cause the workpiece to fracture, as shown in Figure 5c1.

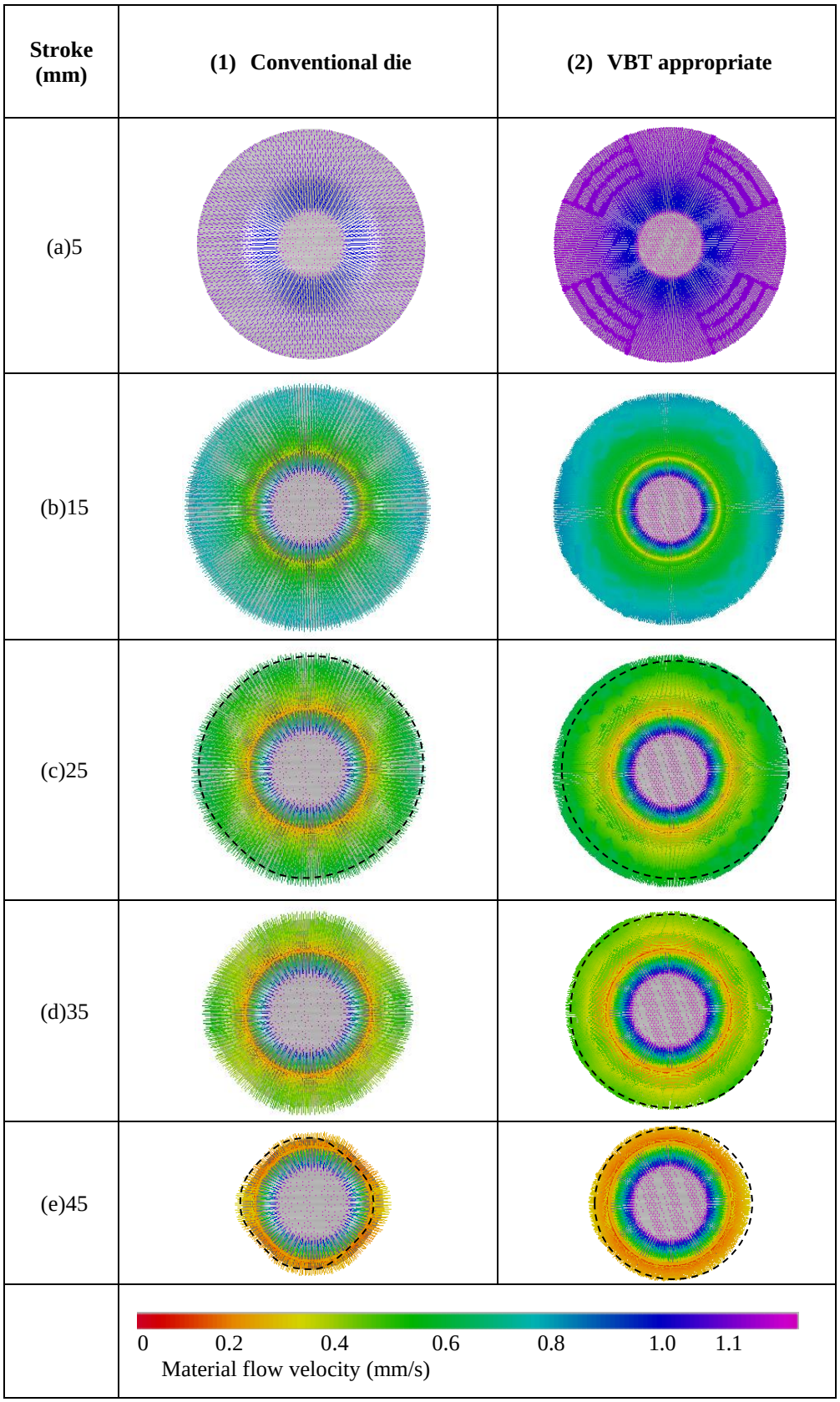

Fig. 4 Comparison of the deep drawing mechanisms between conventional and vertex bar tool-appropriate applications

Stroke (mm)	**VBT Unsuccessful** (VB die and VB blank holder)	
	(1) Higher groove	**(2) Shorter groove**
(a)5	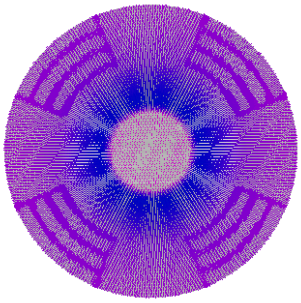	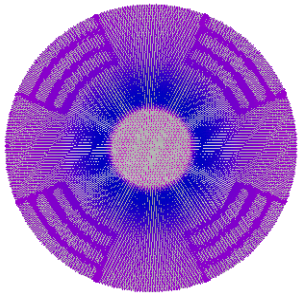
(b)15	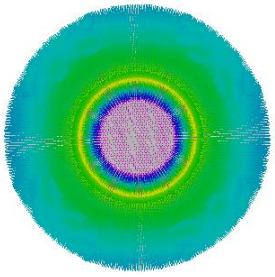	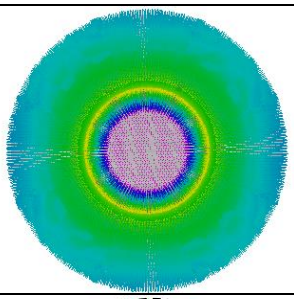
(c)25	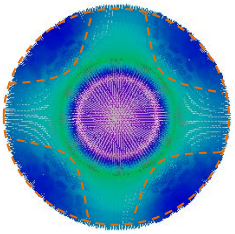	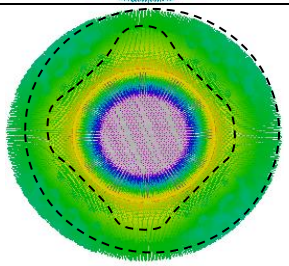
(d)35	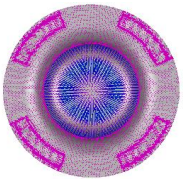	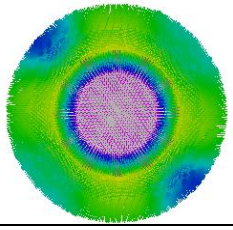
(e)45		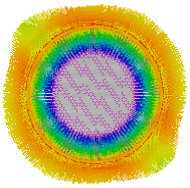
	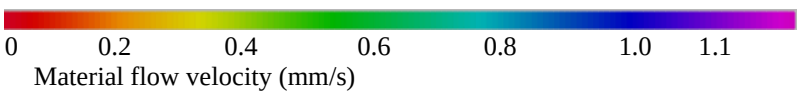	

Fig. 5 Comparison of the deep drawing mechanisms between higher groove and shorter groove vertex bar tool applications

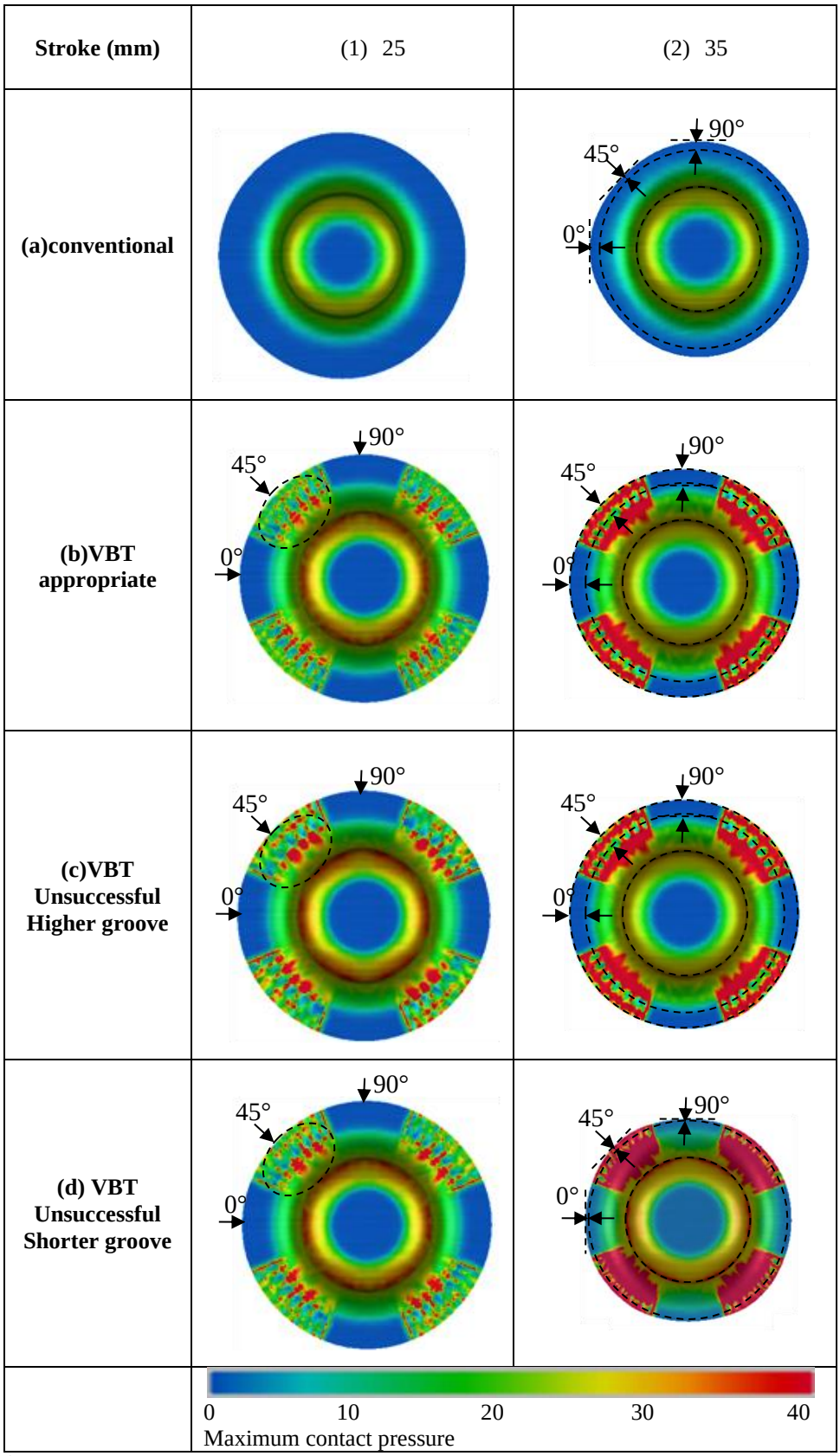

Fig. 6 Comparison of the deep drawing mechanisms maximum contact pressure between conventional, vertex bar tool appropriate, higher groove, and shorter groove vertex bar tool applications

Final part	(1) Finishing deep drawing part		(2) FLD	(3) FLD on part
(a)Conventional die	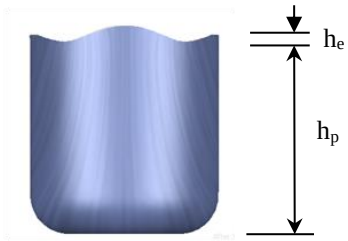		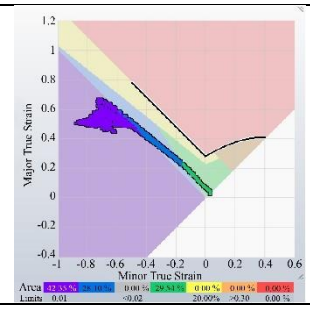	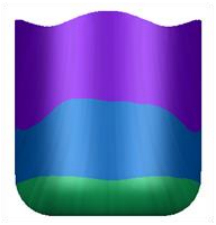
	h_e = 3.6 mm	h_p = 41 mm		
(b)VBT : Appropriate	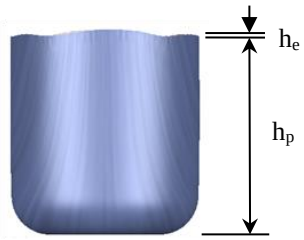		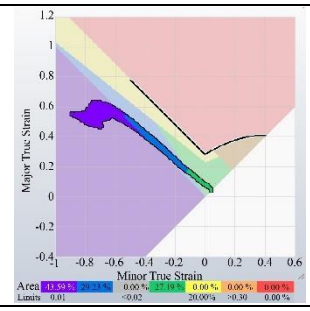	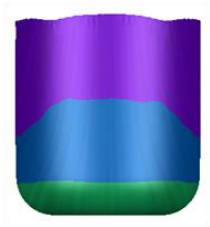
	h_e = 1.6 mm	h_p = 42.5 mm		
(c) VBT : Higher groove	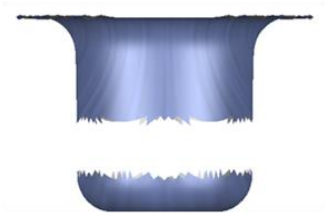		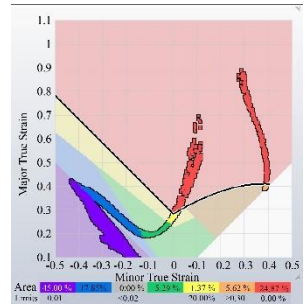	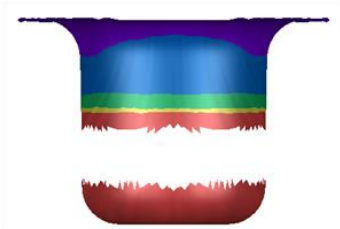
(d) VBT : Shorter groove	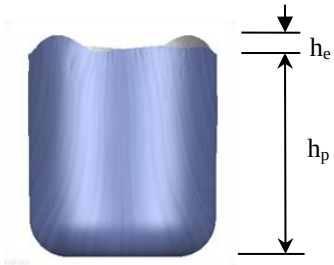		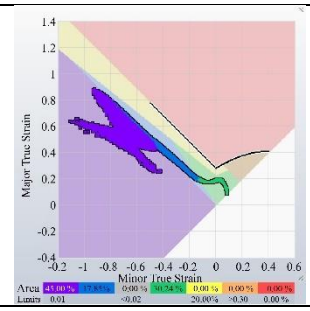	
	h_e = 3.5 mm	h_p = 43.8 mm		

h_e = earring high; h_p= part high

Fig. 7 MDR die design related to the anisotropy property of the material: (a) Conventional die, (b) Vertex bar tool appropriate, (c) Higher groove, and (d) Shorter groove

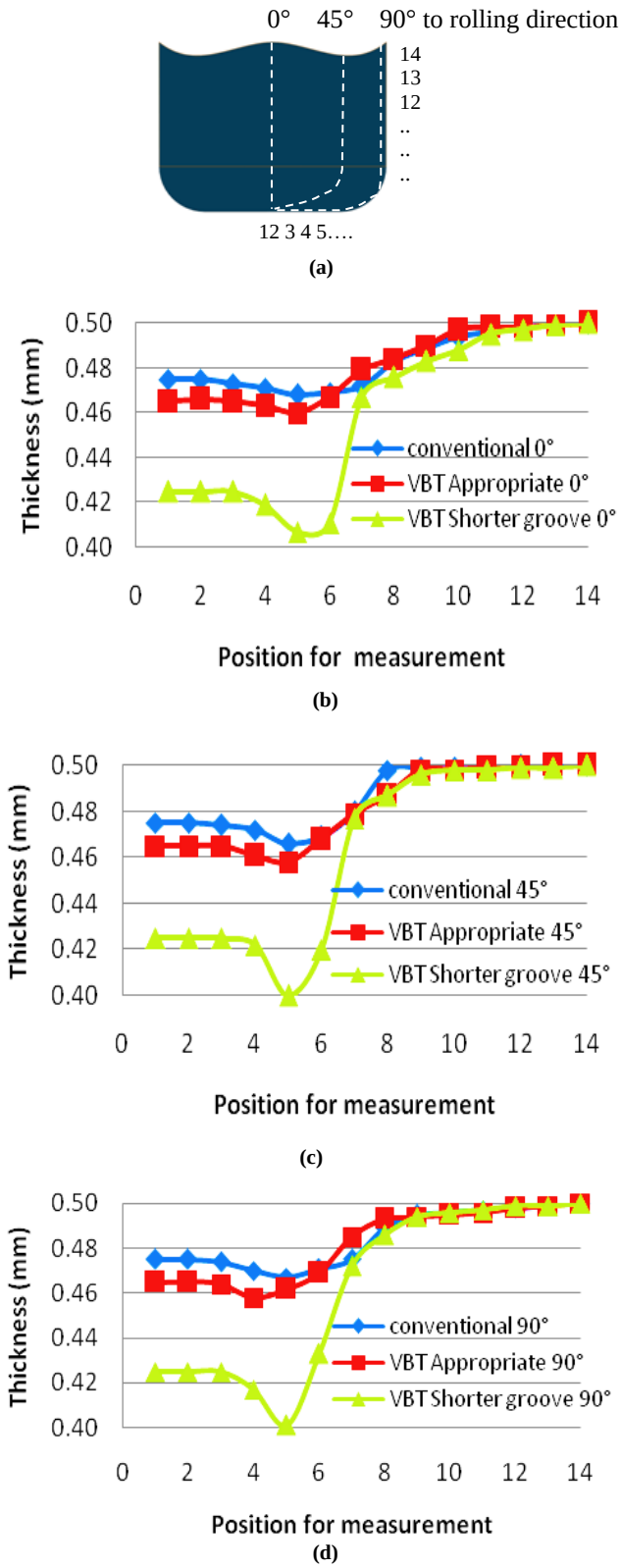

Fig. 8 Cup wall thickness distribution between conventional die, VB Appropriate, and VB Shorter groove at (a) 0° to the rolling direction, (b) 45° to the rolling direction, and (c) 90° to the rolling direction.

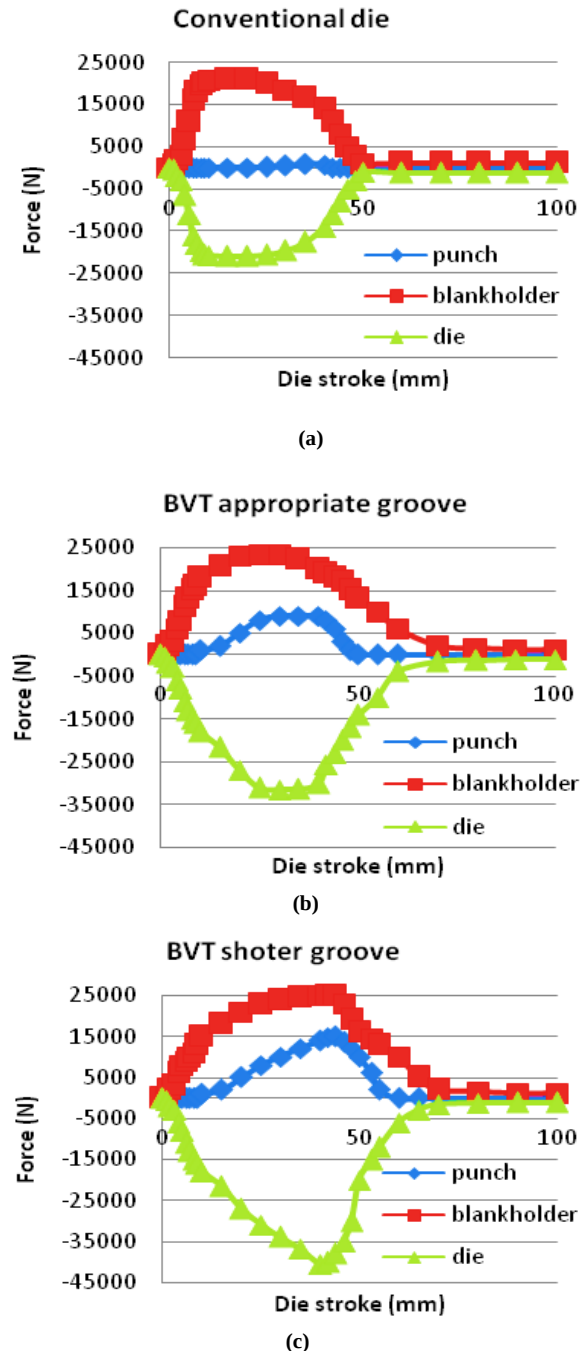

Fig. 9 Comparison of deep drawing force between punch, die, and blankholder with (a) Conventional die, (b) VBT appropriate, and (c) VBT shorter groove.

4.3. Comparison of the Final Part

4.3.1. Thickness Distribution

To validate the accuracy obtained with the conventional die and VB die. VB blank holder applications based on FEM simulations, Figure 8 compares the thickness measurement results taken under three conditions. These conditions are conventional die, VB dies, VB blankholder type appropriate groove, and VB die and VB blankholder type shorter groove.

Based on the three conditions, namely, 0°, 45°, and 90° to the rolling direction, the FEM simulation results show the cup wall thickness of the deep drawing parts. These values are compared in Figures 8a, 8b, and 8c, respectively. The thickness values of the workpieces differed by 2% and 10% between the cases of conventional die and VB die. Blankholder type appropriate groove and conventional die and VB die and blankholder type shorter groove, respectively. The thickness results are satisfactory in the case of VB die and blankholder type appropriate groove.

4.3.2. Deep Drawing Force

Finally, the deep drawing force analyzed by FEM simulation was compared between the three conditions, namely, conventional die, VB die, and blankholder type appropriate groove, and VB die and blankholder type shorter groove, as shown in Figure 9.

5. Conclusion

This research proposed the VB die and VB blankholder method to decrease the earring defect. The design concept is to control the material flow, which is clearly achieved by the VB die and VB blankholder method. FEM simulations were also conducted in this research. The non-axisymmetric material flow characteristic and the flat-top die asymmetry are important factors to consider during the design process. The simulation result obtained using the designed VB die and VB blankholder application demonstrated that the proposed approach effectively controlled the anisotropy property on material flow characteristics at 0°,45°, and 90° rolling direction.

Therefore, the non-axisymmetric material flow characteristic on the flat top die could be controlled to smooth the velocity asymmetry of the flat top die, which mainly affects the core circular initial blank shape. Specifically, the VB die and VB blankholder positioned at 45° to the rolling direction and the flat die and flat blank holder positioned at 0° and 90° to the rolling direction were used. Moreover, the cup wall thickness was considered for the case of VB die and VB blankholder: appropriate groove. Regarding this case, the FEM simulation results predicted a decrease of approximately 0.15% compared with the conventional die results. Finally, the earring defect could be decreased by approximately 55.55% using the VB die and VB blankholder application proposed in this research.

Funding Statement

Funding was also received from the Thailand Science Research and Innovation (TSRI) and Fundamental Fund of Rajamangala University of Technology Rattanakosin with funding under contract No.: A17/2565; project code: 2312643; Research project: Development of sheet-metal forming processes for the next-generation automotive and aviation industries; Fiscal year: 2022

Acknowledgments

The authors would like to specifically thank Professor Sutasn Thipprakmas, Rudeemas Jankree, Saowalak Kongiang, Kongkiet doungmarda, and Jeerawat Sriwirattanakul for their help in this research. The authors would like to express their gratitude to Pravitr Paramaputi, Srisahawattanakij Co. Ltd., for his support in the Cimatron v.3 program.

References

[1] Klaus Pöhlandt, and Kurt Lange, *Handbook of Metal Forming*, McGraw-Hill, pp. 1-900, 1985. [Google Scholar] [Publisher Link]

[2] Wen Sun, Wei Liu, and Shijian Yuan, "Suppressing Wrinkles in Thin-Walled Dome Parts: A Novel Deep Drawing Method with Active Stress Control," *Journal of Materials Processing Technology*, vol. 324, 2024. [CrossRef] [Google Scholar] [Publisher Link]

[3] Sutasn Thipprakmas, "Finite Element Analysis of Sided Coined-Bead Technique in Precision V-Bending Process," *The International Journal of Advanced Manufacturing Technology*, vol. 65, pp. 679-688, 2012. [CrossRef] [Google Scholar] [Publisher Link]

[4] N. Guo et al., "Analysis of Size Dependent Earing Evolution in Micro Deep Drawing of TWIP Steel by Using Crystal Plasticity Modeling," *International Journal of Mechanical Sciences*, vol. 165, 2020. [CrossRef] [Google Scholar] [Publisher Link]

[5] Sutasn Thipprakmas, and Pakkawat Komolruji, "Analysis of Bending Mechanism and Spring-Back Characteristics in the Offset Z-Bending Process," *The International Journal of Advanced Manufacturing Technology,* vol. 85, pp. 2589-2596, 2015. [CrossRef] [Google Scholar] [Publisher Link]

[6] Lade Jayahari et al., "Formability Studies of ASS 304 and Evaluation of Friction for Al in Deep Drawing Setup at Elevated Temperatures using LS-DYNA," *Journal of King Saud University - Engineering Sciences*, vol. 26, no. 1, pp. 21-31, 2014. [CrossRef] [Google Scholar] [Publisher Link]

[7] Yohei Abe, Kai Sugiura, and Ken-ichiro Mori, "Ironing Limit of Aluminium Alloy Cups with Lubricants Containing Nanoparticles and Tool Steel Die," *Procedia Manufacturing*, vol. 50, pp. 114-118, 2020. [CrossRef] [Google Scholar] [Publisher Link]

[8] Can-Bin Zhang, and Feng Gong, "Deep Drawing of Cylindrical Cups Using Polymer Powder Medium Based Flexible Forming," *International Journal of Precision Engineering and Manufacturing-Green Technology*, vol. 5, pp. 63-70, 2018. [CrossRef] [Google Scholar] [Publisher Link]

[9] Bharatkumar Modi, and D. Ravi Kumar, "Optimization of Process Parameters to Enhance Formability of AA 5182 Alloy in Deep Drawing of Square Cups by Hydroforming," *Journal of Mechanical Science and Technology*, vol. 33, pp. 5337-5346, 2019. [CrossRef] [Google Scholar] [Publisher Link]

[10] Wen Zhang, and Jun Xu, "Advance Lightweight Materials for Automobiles: A Review," *Materials & Design*, vol. 221, pp. 1-20, 2022. [CrossRef] [Google Scholar] [Publisher Link]
[11] Wan-Gi Cha et al., "Formability Consideration during Bead Optimisation to Stiffen Deep Drawn Parts," *Production Engineering*, vol. 12, pp. 691-702, 2018. [CrossRef] [Google Scholar] [Publisher Link]
[12] Yohei Abe et al., "Improvement of Sheet Metal Formability by Local Work-Hardening with Punch Indentation," *Production Engineering*, vol. 13, pp. 589-597, 2019. [CrossRef] [Google Scholar] [Publisher Link]
[13] Min Sik Lee et al., "Investigation of Formability and Fiber Orientation in the Square Deep Drawing Process with Steel/CFRP Hybrid Composites," *International Journal of Precision Engineering and Manufacturing*, vol. 20, pp. 2019–2031, 2019. [CrossRef] [Google Scholar] [Publisher Link]
[14] M. Kadkhodayan, and F. Moayyedian, "Analytical Elastic–Plastic Study on Flange Wrinkling in Deep Drawing Process," *Iranian Science*, vol. 18, no. 2, pp. 250-260, 2011. [CrossRef] [Google Scholar] [Publisher Link]
[15] C.J. Wang et al., "Research on Micro-Deep Drawing Process of Concial Part with Ultra-Thin Copper Foil Using Multi-Layered DLC Film-Coated Die," *The International Journal of Advanced Manufacturing Technology*, vol. 100, pp. 569-575, 2018. [CrossRef] [Google Scholar] [Publisher Link]
[16] Liang Luo et al., "Influence of Blank Holder-Die Gap on Micro Drawing of SUS304 Cups," *International Journal of Mechanical Sciences*, vol. 191, 2021. [CrossRef] [Google Scholar] [Publisher Link]
[17] Di Pan et al., "Tribological Behaviour of Ultra-Thin Stainless Steel in Micro Deep Drawing with Graphene Nanosheets," *Wear*, vol. 524-525, 2023. [CrossRef] [Google Scholar] [Publisher Link]
[18] Fanghui Jia et al., "Experimental Study on Drawability of Aluminium-Copper Composite in Micro Deep Drawing," *Journal of Materials Processing Technology*, vol. 307, 2022. [CrossRef] [Google Scholar] [Publisher Link]
[19] Shamik Basak, Sushanta Kumar Panda, and Myoung-Gyu Lee, "Formability and Fracture in Deep Drawing Sheet Metals: Extended Studies for Pre-Strained Anisotropic Thin Sheets," *International Journal of Mechanical Sciences*, vol. 170, 2020. [CrossRef] [Google Scholar] [Publisher Link]
[20] Bernd-Arno Behrens, Hendrik Wester, and Matthäus Dykiert, "Fracture Modelling of Magnesium Sheet Alloy AZ31 for Deep Drawing Processes at Elevated Temperatures," *Procedia Manufacturing*, vol. 50, pp. 739-743, 2020. [CrossRef] [Google Scholar] [Publisher Link]
[21] Haibo Wang et al., "Prediction of Eight Earings in Deep Drawing of 5754O Aluminum Alloy Sheet," *Chinese Journal of Mechanical Engineering*, vol. 32, 2019. [CrossRef] [Google Scholar] [Publisher Link]
[22] Jingwei Zhao et al., "Experimental Investigation on Micro Deep Drawing of Stainless Steel Foils with Different Microstructural Characteristics," *Chinese Journal of Mechanical Engineering*, vol. 34, pp. 1-11, 2021. [CrossRef] [Google Scholar] [Publisher Link]
[23] Kelin Chen, and Yannis P. Korkolis, "Industry 4.0 in Stamping: A Wrinkling Indicator for Reduced-Order Modeling of Deep-Drawing Processes," *Procedia Manufacturing*, vol. 51, pp. 864-869, 2020. [CrossRef] [Google Scholar] [Publisher Link]
[24] Kailun Zheng et al., "A Study on the Buckling Behavior of Aluminum Alloy Sheet in Deep Drawing with Macro-Textured Blankholder," *International Journal of Mechanical Sciences*, vol. 110, pp. 138-150, 2016. [CrossRef] [Google Scholar] [Publisher Link]
[25] Simon Schöler et al., "Investigations of Hot-Dip Galvanized Dual-Phase Steel (DP600+Z) Sheet Metal on Selectively Oxidized Tool Steel Surfaces Under Dry Deep-Drawing Conditions," *Wear*, vol. 484-485, 2021. [CrossRef] [Google Scholar] [Publisher Link]
[26] Ali Mousavi, Michael Schomäcker, and Alexander Brosius, "Macro and Micro Structuring of Deep Drawing's Tools for Lubricant Free Forming," *Procedia Engineering*, vol. 81, pp. 1890-1895, 2014. [CrossRef] [Google Scholar] [Publisher Link]
[27] A. Brosius, and A. Mousavi, "Lubricant Free Deep Drawing Process by Macro Structured Tools," *CIRP Annals*, vol. 65, no. 1, pp. 253-256, 2016. [CrossRef] [Google Scholar] [Publisher Link]
[28] Matthäus Kott et al., "Controllability of Temperature Induced Friction Effects during Deep Drawing of Car Body Parts with High Drawing Depths in Series Production," *Procedia Manufacturing*, vol. 47, pp. 553-560, 2020. [CrossRef] [Google Scholar] [Publisher Link]
[29] Kenza Bouchaâla et al., "Evaluation of the Effect of Contact and Friction on Deep Drawing Formability Analysis for Lightweight Aluminum Lithium Alloy Using Cylindrical Cup," *Procedia Manufacturing*, vol. 46, pp. 623-629, 2020. [CrossRef] [Google Scholar] [Publisher Link]
[30] Emir Hodžić et al., "Influence of Alloy Composition and Lubrication on the Formability of Al-Mg-Si Alloy Blanks," *Journal of Manufacturing Processes*, vol. 85, pp. 109-121, 2023. [CrossRef] [Google Scholar] [Publisher Link]
[31] Gerd Reichardt, and Mathias Liewald, "Investigation on Friction Behaviour of Deep Drawing Radii Using Volatile Media as Lubricant Substitutes," *Procedia Manufacturing*, vol. 29, pp. 193-200, 2019. [CrossRef] [Google Scholar] [Publisher Link]